Supporting Information

High-Performance Lead-free Piezoelectrics with Local Structural Heterogeneity

Qing Liu[1] , Yichi Zhang[1], Jing Gao[1], Zhen Zhou[1], Hui Wang[2], Ke Wang[1] , Xiaowen Zhang[1], Longtu Li[1], and Jing-Feng Li[1]**

[1]State Key Laboratory of New Ceramics and Fine Processing, School of Materials Science and Engineering, Tsinghua University, Beijing 100084, China

[2]Key Laboratory of Aerospace Materials and Performance (Ministry of Education), School of Materials Science and Engineering, Beihang University, Beijing 100191, China

* Corresponding author:
jingfeng@mail.tsinghua.edu.cn (Jing-Feng Li)
yichi-zhang@mail.tsinghua.edu.cn (Yichi Zhang)

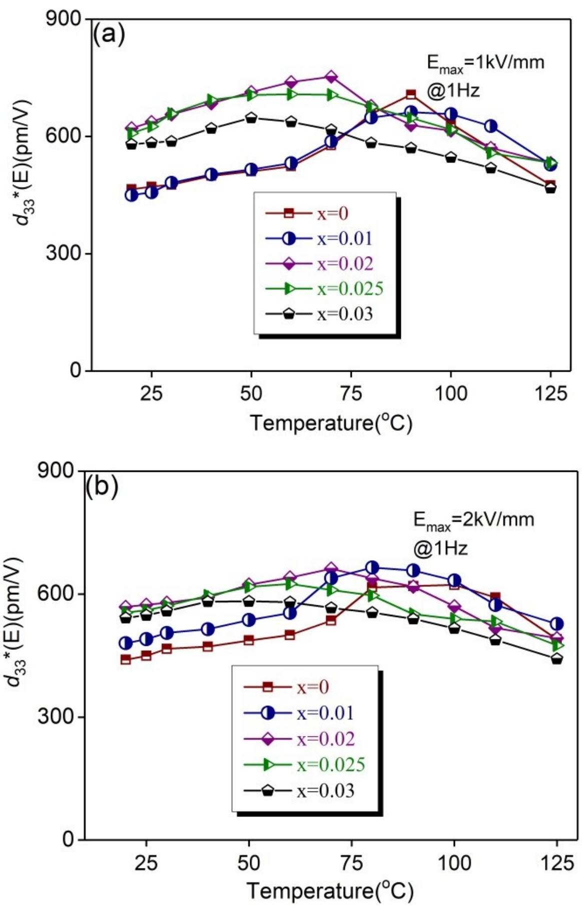

Figure S1. The temperature stability of the d_{33}^* calculated by S_{max}/E_{max}, E_{max}=1kV/mm (a) and E_{max}=2kV/mm (b) for the $KNNS_x$-5BZ-2BNH-1Mn samples.

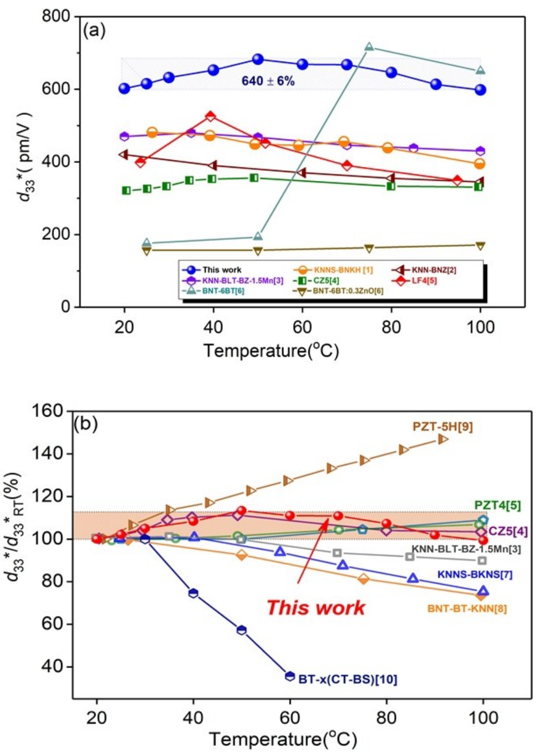

Figure S2. (a).Comparison of piezoelectric strain coefficient d_{33}^* from room temperature to 100 ^oC under certain electric fields of several representative systems. [1-6] (b). Comparison of the temperature dependences of large signal d_{33}^* for various ceramics as normalized to its room temperature value $d_{33}^*{}_{RT}$. [3-5, 7-10]

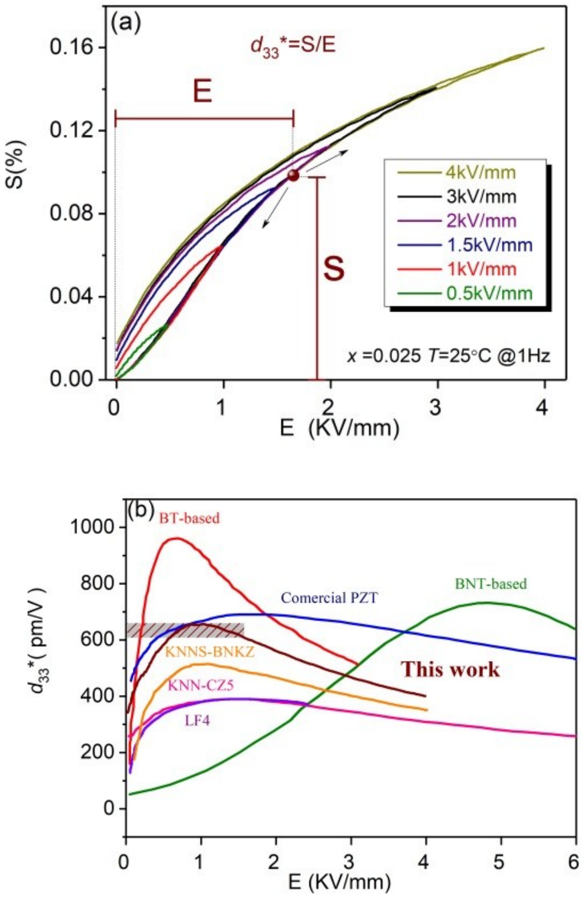

Figure S3. (a) Unipolar electric-field-induced strain curves for the *x*=0.025 sample under different electric fields. (b) The converse d_{33}* at room temperature as a function of field for this work and other representative lead-free piezoelectric as well as commercial PZT (PIC 151). [4, 5, 7, 11-16]

To give further insights into the relationship between d_{33}^* and electric field, the converse d_{33}^* as a function of electric field was calculated by S/E according to the S-E curve measured under a triangular-shaped base waveform with E_{max}=4kV/mm at room temperature for this work as shown in **Figure S3(a)**, and the relationship between d_{33}^* and electric field for other representative lead-free piezoelectrics as well as commercial PZT (PIC 151) were obtained from literature as shown in **Figure S3(b)**. [4, [5, 7, 11-16] A large d_{33}^* above 600pm/V could be obtained at the low electric field (1 kV/mm ≤ E ≤ 1.5kV/mm) in this work , which is in analogy with PZT , while a larger driving electric field is expected in BNT-based ceramics. [17] BT-based ceramics show a higher level d_{33}^* but the application temperature range could be limited by their low T_c . Considering the high level of the d_{33}^* and the reliable feature in analogy with PZT, this material exhibits the promising potential in the actuator applications.

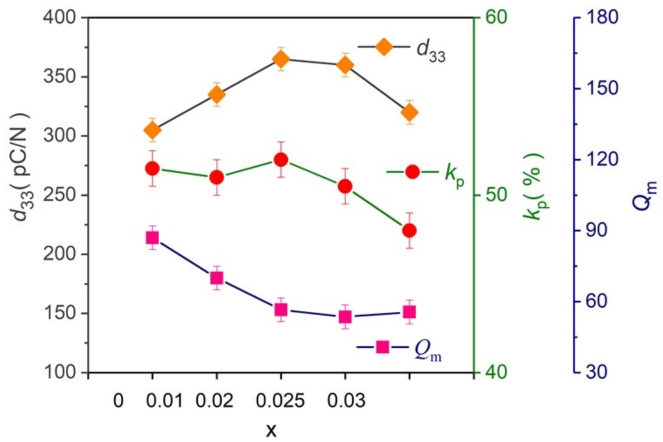

Figure S4. Planar electro-mechanical coupling factor k_p, piezoelectric voltage coefficient d_{33} and the mechanical quality factor Q_m of of poled KNNSx-5BZ-2BNH ceramics.

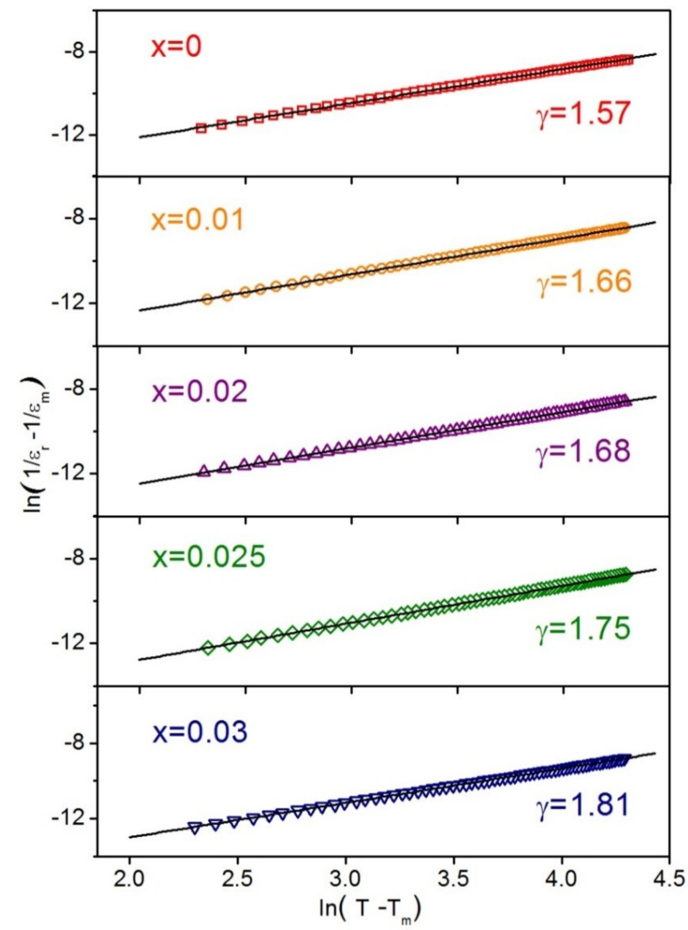

Figure S5. In($1/\varepsilon$-$1/\varepsilon_m$) vs. In(T-T_m) figures of the KNNS$_x$-BBNZH-1Mn samples for determining the calculated degree of diffuseness γ.

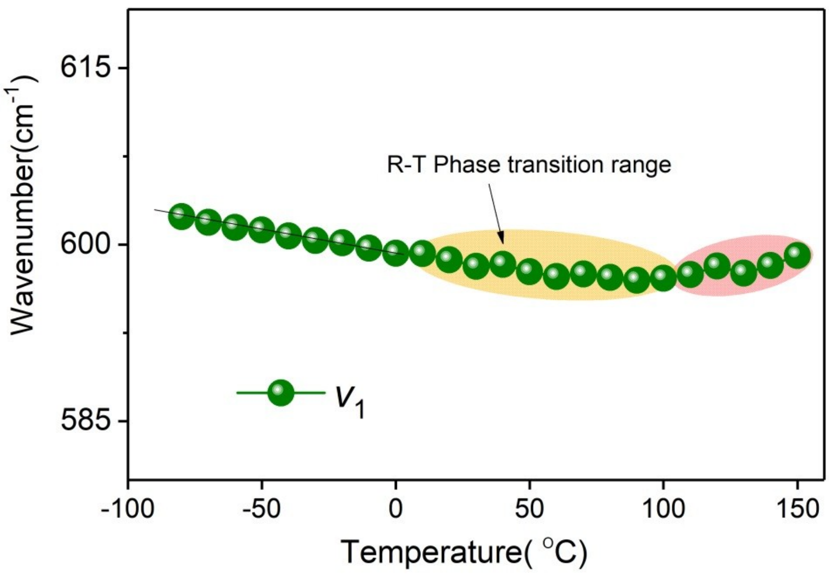

Figure S6. The temperature dependence of the v_1 peak positions.

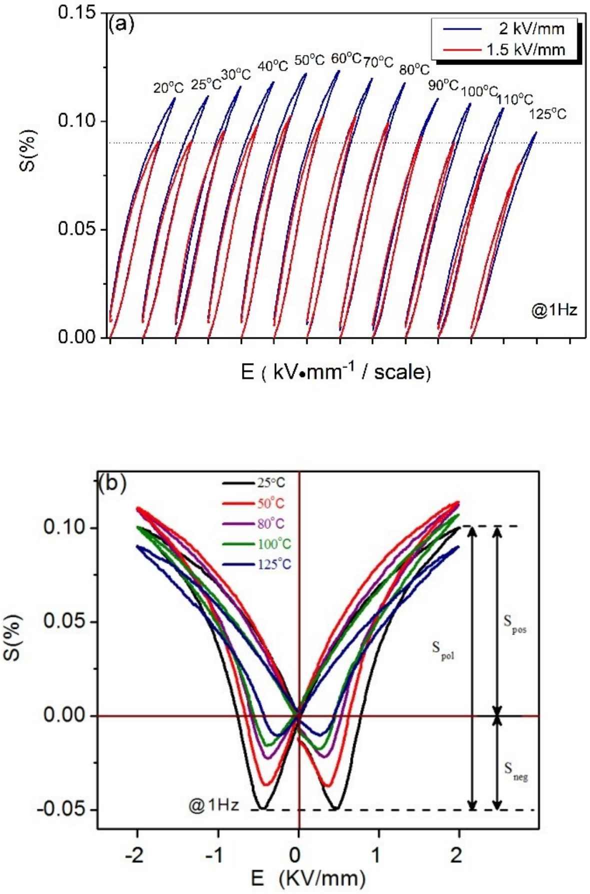

Figure S7. (a) Unipolar electric-field-induced strains under different electric fields (E_{max}=1.5kV/mm and 2kV/mm) in the temperature range 20-125^{o}C for the *x*=0.025 sample. (b) Bi-polar electric-field-induced strain curves of the *x*=0.025 sample under a triangular-shaped base waveform with a maximum electric field 2kV/mm.

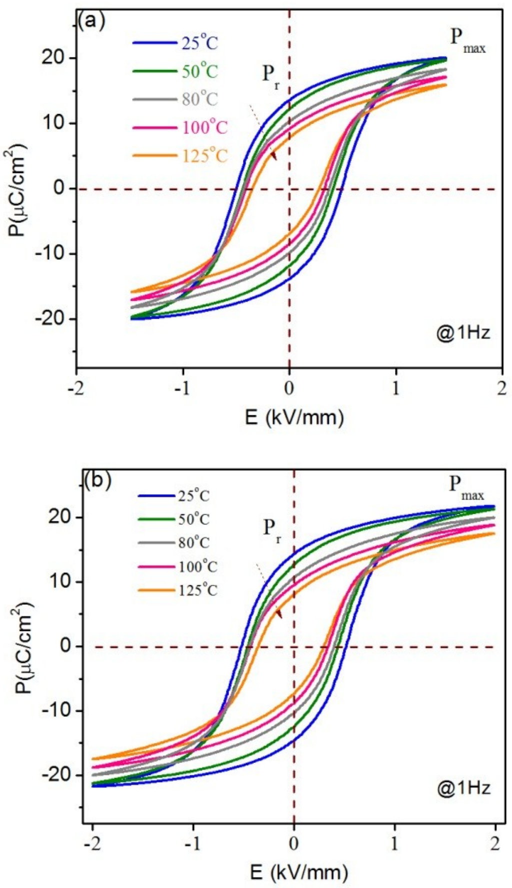

Figure S8. *P*-*E* loops for x=0.025 sample under electric fields with E_{max}=1.5 kV/mm (a) and E_{max}= 2 kV/mm.

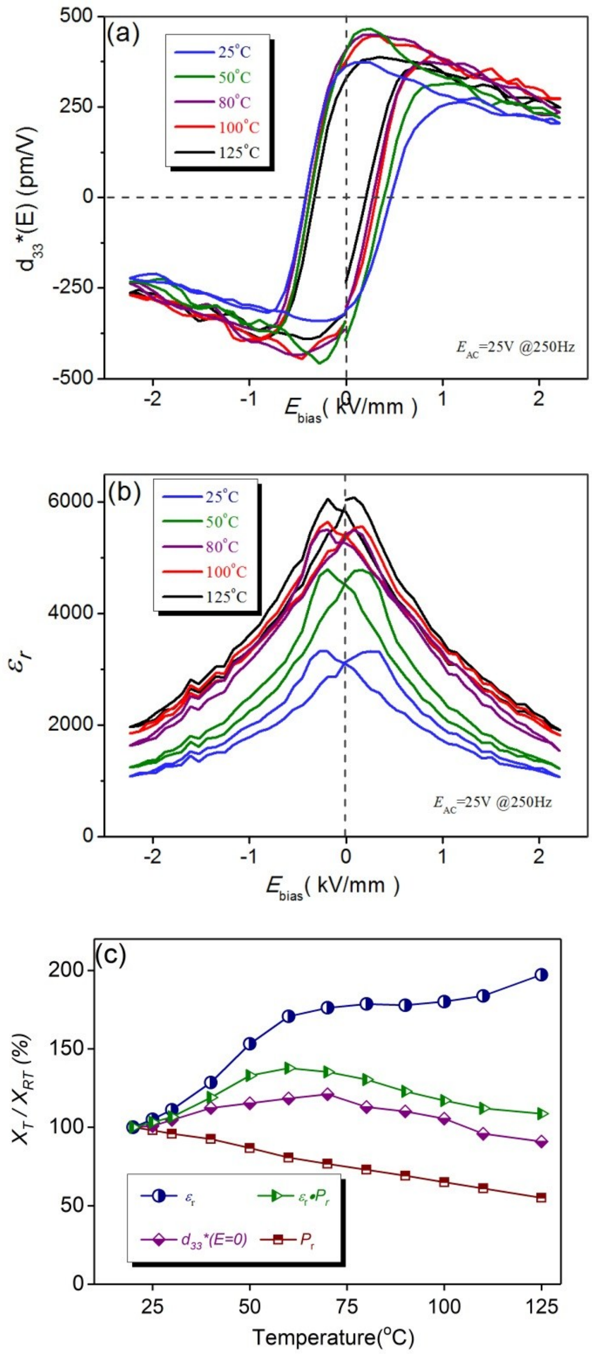

Figure S9. (a) $d_{33}{}^{*}$(E) hysteresis loops at different temperatures for the *x*=0.025 sample.(b) ε_r -E_{bias} curves at different temperatures.(c) Summary of the temperature dependence of the relative dielectric coefficient ε_r , remanent polarization P_r , ε_r•P_r and the small signal $d_{33}{}^{*}(E=0)$.

The small signal d_{33} exhibits a strong relationship with dielectric and ferroelectric properties as written in the equation: [1, 18-21]

$d_{33} \sim \alpha\varepsilon_r \bullet P_r$.

The temperature dependence of small signal d_{33} is almost in tune with the variation of $\varepsilon_r \bullet P_r$. It is considered that the good thermal stability of small signal d_{33} should be attributed to the balance between reduced P_r and enhanced dielectric property due to the phase transition.

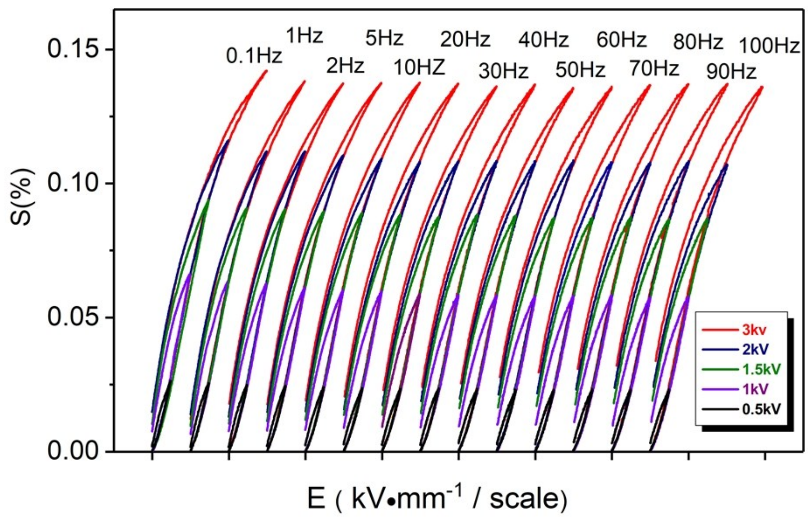

Figure S10. The S-E curves of the x=0.025 sample measured at different frequencies and electric fields.

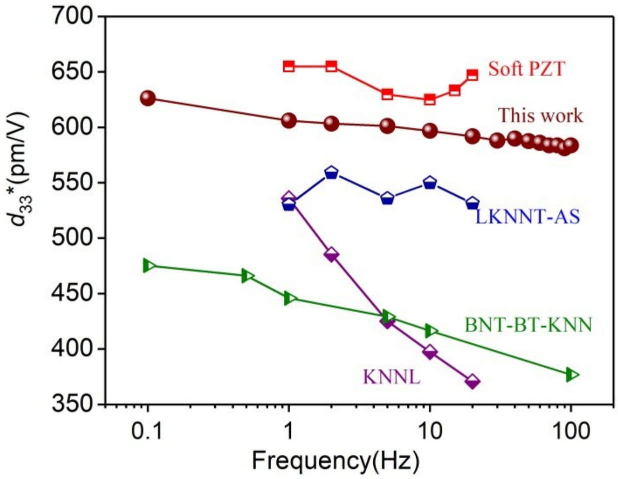

Figure S11. Frequency dependence d_{33}^* of the optimal composition in this work compared with that of KNN-based ceramics, typical BNT-based ceramics and soft PZT as reported in References. [22-24]

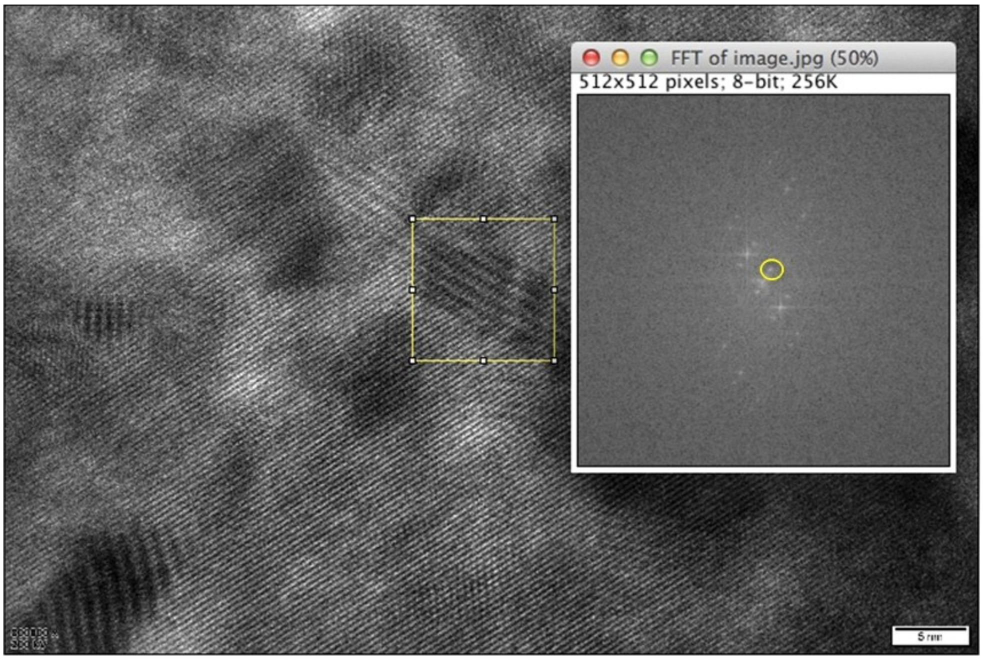

Figure S12. Fast Fourier transform (FFT) of a selected nanosized pattern showing moiré fringes. The diffraction spot indicated by the yellow circle is corresponding to the periodicity of the fringes inside the pattern.

Reference

[1] T. Zheng, H. Wu,Y. Yuan, X. Lv, Q. Li, T. Men, C. Zhao, D. Xiao, J. Wu, K. Wang, J.-F. Li,Y. Gu, J. Zhu, S. J. Pennycook , *Energ. Environ. Sci.* **2017**, 10, 528.

[2] D. Wang, F. Hussain, A. Khesro, A. Feteira, Y. Tian, Q. Zhao, I. M. Reaney, *J. Am. Ceram. Soc.* **2017**, 100, 627.

[3] M.-H. Zhang, K. Wang, Y.-J. Du, G. Dai, W. Sun, G. Li, D. Hu, H. C. Thong, C. Zhao, X.-Q. Xi, Z.-X. Yue ,J.-F. Li, *J. Am. Chem. Soc.* **2017**, 139, 3889.

[4] K. Wang, F.-Z. Yao, W. Jo, D. Gobeljic, V. V. Shvartsman, D. C. Lupascu, J.-F. Li, J. Rödel, *Adv. Funct. Mater.* **2013**, 23, 4079.

[5]Y. Saito, H. Takao, T. Tani, T. Nonoyama, K. Takatori, T. Homma, T. Nagaya, M. Nakamura, *Nature* **2004**, 432, 84.

[6] J. Zhang, Z. Pan, F.-F. Guo, W.-C. Liu, H. Ning, Y. Chen, M.-H. Lu, B. Yang, J. Chen, S.-T. Zhang, *Nat. commun.* **2015**, 6.

[7] J.-S. Zhou, K. Wang, F.-Z. Yao, T. Zheng, J. Wu, D. Xiao, J. Zhu, J.-F. Li, *J. Mater. Chem. C* **2015**, 3, 8780.

[8] S.-T. Zhang, A. B. Kounga, E. Aulbach , *J. Appl. Phys* **2008**. 103(3), 034108.

[9]D. Wang, Y. Fotinich, G.P. Carman, *J. Appl. Phys.* **1998**. 83(10), 5342-5350.

[10] L.-F. Zhu, B.-P. Zhang, L. Zhao and J.-F. Li, *J. Mater. Chem. C*, **2014**, 2, 4764.

[11]M. Senousy, R. Rajapakse, D. Mumford, M. Gadala, *Smart Mater. Struct.* **2009**, 18, 045008.

[12] R. Dittmer, W. Jo, J. Daniels, S. Schaab, J. Rödel, *J. Am. Ceram. Soc.* **2011**, 94, 4283.

[13] A. Hussain, J. U. Rahman, A. Zaman, R. A. Malik, J. S. Kim, T. K. Song, W. J. Kim, M. H. Kim, *Mater. Chem. Phys.* **2014**, 143, 1282.

[14] W. Jo, E. Erdem, R.-A. Eichel, J. Glaum, T. Granzow, D. Damjanovic, J. Rödel, *J. Appl. Phys*. **2010**, 108, 014110.

[15] M. Acosta, N. Novak, W. Jo, J. Rödel, *Acta Mater.* **2014**, 80, 48.

[16]Y. Qin, J. Zhang, W. Yao, C. Lu, S. Zhang, *ACS Appl. Mater. Int.* **2016**, 8, 7257.

[17] M. Acosta, L. A. Schmitt, L. Molina‐Luna, M. C. Scherrer, M. Brilz, K. G. Webber, M. Deluca, H. J. Kleebe, J. Rödel, W. Donner, *J. Am. Ceram. Soc.* **2015**, 98, 3405.

[18]K. Xu, J. Li, X. Lv, J. Wu, X. Zhang, D. Xiao, J. Zhu, *Adv. Mater.* **2016**, 28, 8519.

[19] J. Wu, D. Xiao, J. Zhu, *Chem. Rev.* **2015**, 115, 2559.

[20] X. Wang, J. Wu, D. Xiao, J. Zhu, X. Cheng, T. Zheng, B. Zhang, X. Lou, X. Wang, *J. Am. Chem. Soc.* **2014**, 136, 2905.

[21]T. R. Shrout, S. J. Zhang, *J. Electroceram.* **2007**, 19, 113.

[22]J. J. Zhou, K. Wang, F. Li, J. F. Li, X. W. Zhang, Q. M. Wang, *J. Am. Ceram. Soc.* **2013**, 96, 519.

[23] W. Jo, R. Dittmer, M. Acosta, J. Zang, C. Groh, E. Sapper, K. Wang, J. Rödel, *J. Electroceram.* **2012**, 29, 71.

[24]K. Wang, J.-F. Li, J.-J. Zhou, *Appl. Phys. Express* **2011**, 4, 061501.